Detection and Discrimination of Motion-Defined Form: Implications for the Use of Night Vision Devices

Robert S. Allison, *Senior Member, IEEE*, Todd Macuda, and Sion Jennings

***Abstract*—Superimposed luminance noise is typical of imagery from devices used for low-light vision such as image intensifiers (i.e., night vision devices). In four experiments, we measured the ability to detect and discriminate motion-defined forms as a function of stimulus signal-to-noise ratio at a variety of stimulus speeds. For each trial, observers were shown a pair of image sequences—one containing dots in a central motion-defined target region that moves coherently against the surrounding dots, which moved in the opposite or in random directions, while the other sequence had the same random/uniform motion in both the center and surrounding parts. They indicated which interval contained the target stimulus in a two-interval forced-choice procedure. In the first experiment, simulated night vision images were presented with Poisson-distributed spatiotemporal image noise added to both the target and surrounding regions of the display. As the power of spatiotemporal noise was increased, it became harder for observers to detect the target, particularly at the lowest and highest dot speeds. The second experiment confirmed that these effects also occurred with low illumination in real night vision device imagery, a situation that produces similar image noise. The third experiment demonstrated that these effects generalized to Gaussian noise distributions and noise created by spatiotemporal decorrelation. In the fourth experiment, we found similar speed-dependent effects of luminance noise for the discrimination (as opposed to detection) of the shape of a motion-defined form. The results are discussed in terms of physiological motion processing and for the usability of enhanced vision displays under noisy conditions.**

***Index Terms*—Human factors, image intensifiers, motion perception, night vision, noise.**

I. Introduction

RELATIVE motion provides a powerful cue for form detection and segregation from background. Camouflage by texture matching to the background can be so effective that many insects and other creatures can often only be seen based on relative motion between the animal and the background. Thus, the ability to detect a camouflaged form based on motion is important in the natural ecology of predator–prey relationships and in other settings such as helicopter flight or military surveillance. In the laboratory, we can carefully remove other cues for discerning form and demonstrate that form perception can be based on relative motion alone [1]. The processing of motion-defined form relies on segregation of motion information within the hidden entity from the background based on differences in the motion signal. At low luminance and in some optical instruments, the motion signal is degraded by image noise. The noise can be added by the electronics or may be due to the basic physical properties of light (for instance the quantal nature of photon arrival statistics at the retina becomes evident at low light levels [2]). In this paper we ask, what is the effect of spatiotemporal luminance noise on the detection and discrimination of the motion-defined form?

One practical example of where luminance noise may influence visual performance is in night vision devices (NVDs). In aviation, nght vision goggles (NVGs) and other NVDs allow pilots to see and navigate under minimal levels of illumination by amplifying the available light. Although NVDs enhance night vision, their visual effects have been implicated as a causal factor in military helicopter incidents and accidents in a number of countries. Indeed, some reports have identified the risk of night flying with NVDs to be 10–15 times greater than for ordinary daytime flight [3], [4].

Noise is an inescapable phenomenon of electric-optical devices, such as NVDs, that operate near limits. While the NVDs amplify available light, they also create scintillating noise under very low light conditions. This scintillation degrades the image quality producing a "grainy" appearance. Reducing the input light level increases the relative magnitude and contribution of this visual noise. Anecdotal reports suggest that this NVD image noise affects visual processing (e.g., acuity, motion, texture, and depth perception) and this degradation may play a role in the increased incident and accident rates noted previously.

Although Durgin and Proffitt [5], [6] found no effect of NVD image noise on judgments of texture density, the signal-to-noise ratio (SNR) of NVDs has been shown to influence visual acuity [7], [8]. It is possible that noise may differentially affect visual processing, leaving some processes such as texture discrimination unaffected while impairing acuity, depth, and motion perception as noise levels increase.

Manuscript received February 1, 2013; revised June 11, 2013 and September 19, 2013; accepted September 21, 2013. Date of publication October 23, 2013; date of current version November 26, 2013. This work was supported by the Center for Research in Earth and Space Technology (CRESTech). This paper was recommended by Associate Editor M. Dorneich.

R. S. Allison is with the Department of Electrical Engineering and Computer Science, Centre for Vision Research, York University, Toronto, ON M3J 1P3, Canada (e-mail: allison@cse.yorku.ca).

T. Macuda was with the Flight Research Laboratory, National Research Council of Canada, Ottawa, ON K1A 0R6, Canada and the Centre for Vision Research, York University, Toronto, ON M3J 1P3, Canada. He is now with Malmacinternational, Ottawa, ON K2K 2G5, Canada (e-mail: toddjmacuda@gmail.com).

S. Jennings is with the Flight Research Laboratory, National Research Council of Canada, Ottawa, ON K1A 0R6, Canada (e-mail: Sion.Jennings@nrc-cnrc.gc.ca).

Color versions of one or more of the figures in this paper are available online at http://ieeexplore.ieee.org.

Digital Object Identifier 10.1109/THMS.2013.2284911

In this paper, we use physical models of NVD image noise to determine its effect on motion perception. Although there have been compelling anecdotal reports of impaired motion perception this is the first systematic study of the impact of NVD scintillation on processing of form from motion. In the first experiment, we show that the capacity to detect motion-defined form is impaired under simulated low levels of illumination. In the second experiment, we confirm this finding by comparing the capacity to detect motion-defined form under simulated and real NVD conditions. We then show that these findings generalize to other noise distributions (see Experiment 3) and to the discrimination of motion-defined form as well as detection (see Experiment 4).

II. General Methods

A. Participants

Four observers (two males, two females) participated in Experiment 1, two observers (one male, one female) participated in Experiment 2, five observers (four male, one female) participated in Experiment 3, and two observers (one male, one female) participated in Experiment 4. All observers had normal or corrected-to-normal vision (20/20 or better). Observers were naïve with respect to the purposes of the experiments except for one observer in Experiments 3 and 4 who was an author. Participation in this study was wholly voluntary. The Research Ethics Boards of the National Research Council and York University approved all testing protocols.

B. Apparatus

A Clinton M20ECD5RE monochrome 19″ monitor (Clinton Electronics Corporation, IL, USA) with short persistence, p104 phosphor was used to display the experimental stimuli. The display subtended 17° × 12.8° and had a resolution of 1024 × 768 pixels and a refresh rate of 100 Hz. A Macintosh G4-dual processor computer was used to control the presentation of the test stimuli and to record the observer's responses. Observers were seated at a viewing distance of 1.2 m with their head stabilized on a chin rest (see Fig. 1).

Fig. 1. Experimental setup. Observers viewed the display with natural vision or through night-vision devices at a distance of 120 cm with head stabilized with a chin rest. Black card and material used to block and baffle light has been removed for better visibility of the apparatus.

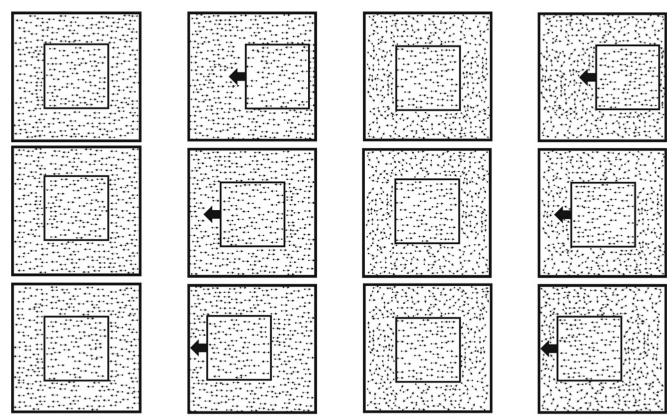

Fig. 2. Schematic view of the stimulus configurations used in Experiment 1. Each row shows how dots move (arrows indicate the instantaneous direction of the dot) on successive frames of the stimulus. The first and third columns depict the stationary border, opposite surround (SBOS) and the stationary border, random surround (SBRS) conditions, respectively. The second and fourth columns show the moving border, opposite surround (MBOS) and the moving border, random surround (MBRS) conditions, respectively.

C. Stimuli

Stimuli consisted of 4000 moving, antialiased dots displayed in a square region (subtending 8.6° × 8.6°). We created motion-defined targets by moving one patch of 1000 dots in a different direction to the remaining dots. This patch was in the center of the display and subtended 4.3° × 4.3° except in Experiment 4, where its aspect ratio varied. The dots were 2 pixels in diameter. If the difference in velocity between the dots in the central patch and the surrounding dots exceeded a certain threshold, the form of the motion-defined region (i.e., in this case a square) was visible. Dots persisted and moved at their specified speed and direction for the duration of the trial (see below for dot behavior at the edges of the regions).

In Experiment 1, four different types of motion-defined-form stimuli were used (see Fig. 2). The first and third columns depict the stationary border, opposing surround (SBOS) and stationary border, random surround (SBRS) conditions, respectively. Under the stationary border conditions, the edges of the motion-defined region remained stationary, while the dots in the target region translated. The dots in the surround region either moved randomly (SBRS) or uniformly in the opposite direction to the motion of the central dots (SBOS). The central and surround dots moved at the same speed and only the direction varied. The perceptual impression of this stimulus was of looking through a square window at dots moving in the background. The second and fourth columns show the moving border, opposing surround (MBOS) and moving border, random surround (MBRS) motion-defined square conditions, respectively. Under these conditions, the edges of the motion-defined region moved with the dots contained within it. The perceptual impression was that of a square in the foreground moving in front of the background.

Dots traveling beyond the limits of the stimulus or border of the central region were replaced (on the opposite side from where they disappeared) to maintain a uniform dot density across the screen. In Experiments 2–4, only the SBRS condition was used.

Four different directions of target area dot motion were used (up, down, left, and right). The direction was randomly selected on each trial. It is important to note that in all stimulus conditions the stimuli were two-dimensional (2-D) and did not contain stereoscopic or other cues to depth (other than differential motion). These images were rendered in Open GL and displayed at 60% Michelson contrast in the absence of noise (64 cd/m^2 dots on a 16 cd/m^2 background). Several different dot speeds were used: 10.1, 20.1, 50.4, 100.7, 201.4, 302.1, 352.5, 402.9, 805.7, 1208.6, and 1611.4 arcmin/s depending on the experiment. The frame rate was 100 frames/s and stimulus duration was 250 ms (Experiments 1 and 2) or 100 ms (Experiments 3 and 4).

D. Night Vision Devices Simulation

Simulated NVD image noise was added to these motion-defined square stimuli using Thomas *et al.*'s [9] model of an NVD. This model incorporates elements for noise and artifact simulation at multiple NVD stages and with varying levels of fidelity. For this paper, we modeled only the Poisson process noise of the photon arrival/electron generation events and the automatic gain control (AGC)/automatic brightness control (ABC) in the device. At the levels of illumination simulated, the Poisson noise is the dominant noise source and isolating it allowed for a clearer interpretation of its effects. We adjusted the intensity of the images that result from the simulated NVD input process to mimic the AGC implemented in typical devices. This process normalized the output light levels so that the mean intensity of the experimental image did not vary with the simulated input illumination.

Image noise was added to both regions of the stimulus. The noise resulted *implicitly* from the model response to a range of input illuminations from full moonlight to cloudy starlight conditions. Bradley and Kaiser's [10] NVIS radiance values for direct illumination of white paper and green leaves were used to select the range of input light levels for our high contrast stimuli. In an NVD, the spacing of the microchannel plate pores determines the spatial sampling of the image intensifier tube and thus the pores are analogous to the pixels in our stimuli. The NVIS radiance values were used to calculate the photons per microchannel plate pore (each pixel represented a pore with simulated quantum efficiency of 10%) per 10-ms time frame to be entered into our model and create a realistic range of noise in the image.

The noise power was expressed in terms of the variance (power) of the Poisson random process that describes the photon arrival, which depends on the intensity of the dots and background. The SNR was calculated from the noise model as the ratio of the signal power (square of the difference in average signal level between the bright dots and dark background) to the root-mean-square noise power in the background.

E. Procedure

The procedure was similar for the first three experiments. On each trial, an observer viewed two consecutive displays separated by a 500-ms delay during which a blank screen was shown. One presentation contained a motion-defined square with image noise, while the other contained only the surround dot motion (i.e., the same uniform or random motion across the entire image) and image noise. The same level of noise was used for both the distracter and target stimulus in a given trial. The order in which the target and distracter were presented was randomized across trials. The observer was required to report whether the stimulus (i.e., the square) was presented in the first or second interval by pushing the keypad number "1" or "2", respectively. If the observer was uncertain when the square appeared they were instructed to make their best guess in a two-interval forced choice procedure (2-IFC). Because there are two available choices for each test trial, pure guessing resulted in a "chance" level of performance of 50%. Observers received at least 150 trials of preliminary training on this 2-IFC procedure that included several image noise levels and methods of producing motion-defined squares.

Within each session, a method of constant stimuli was used to obtain the psychometric functions. In each session, observers were presented with repetitions of each of the noise–speed combinations in random order. The motion or viewing conditions were counterbalanced between sessions. Testing proceeded until observers had completed at least 20 trials on each noise–speed combination for each motion or viewing condition in a given experiment (a minimum of 2400 trials per observer). Observers participated in one session per day at approximately the same time each day (the number of sessions depended on the amount of data required for each experiment, see below).

III. Experiment 1: Detection of a Motion-Defined Form in the Presence of Synthetic Noise

In the first experiment, we used physics-based simulations of NVD noise to investigate the effects of noise on motion-defined form perception.

A. Methods

Observers detected SBOS, SBRS, MBOS, and MBRS motion-defined squares in a 2-IFC procedure as described in Section II. The dot speeds tested were 20.1, 50.4, 100.7, 201.4, and 302.1 arcmin/s. Seven input light levels of 100, 233, 367, 500, 667, 833, and 1000 photons per pore/pixel per frame (for the white dots) were used. The corresponding SNR (see Section II) were 0.23, 0.52, 0.83, 1.13, 1.50, 1.87, and 2.25.

B. Results and Discussion

Fig. 3 shows the total percentage of correct target detections, as a function of dot speed at each image intensity, averaged over the observers for each of the SBOS, SBRS, MBOS, and MBRS conditions, and pooled across the four motion conditions. Each of the curves in this figure represents a different image SNR based on the illumination intensities (i.e., photons per pore per

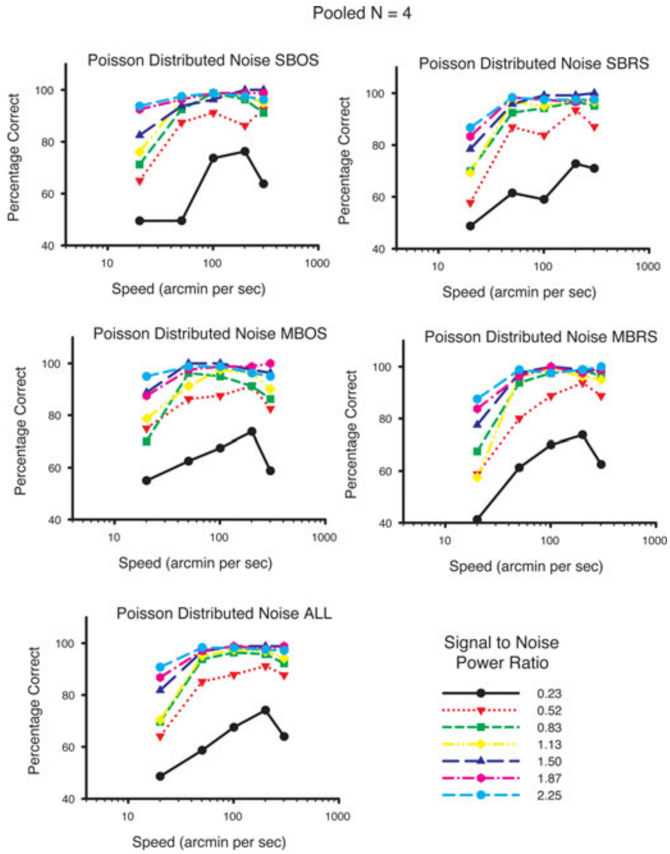

Fig. 3. Motion-defined square detection performance pooled over observer for each motion type and, in the last panel, pooled across motion type. Each curve represents percentage correct detection for a different signal to noise ratio condition as a function of dot speed.

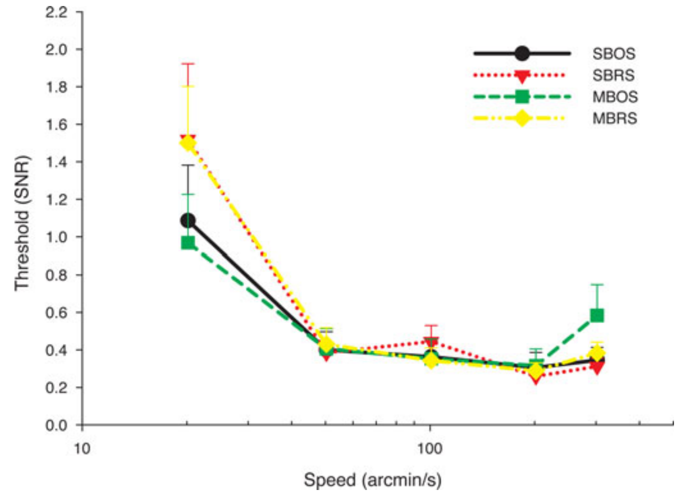

Fig. 4. Threshold image SNR plotted as a function of dot speed for the four motion-defined form types. Error bars represent one standard error of the mean across observers (shown in the positive direction only to minimize clutter).

frame). Thus, a lower value is equivalent to a higher image noise level.

Detection performance decreased as the image noise increased (i.e., as the modeled input illumination level was reduced). Thus, observers had difficulty detecting the square as the image noise was increased. However, performance was generally near perfect at the middle dot speeds for all but the two lowest SNR. For all observers and in the mean data, performance was consistently poorest across all dot speeds at the lowest SNR of 0.23.

Poorer performance was also demonstrated at lower dot speeds. However, even at the lowest speed, the detection performance for the two lowest noise levels exceeded 90%. This indicates that observers could perform the task, and it was not the case where the absolute dot speeds were below threshold for motion-defined form detection. As the motion contrast signal was weakened by slower dot speed though, performance appeared to be more susceptible to image noise. The effects of noise also appeared more pronounced at higher speeds. Thus, the effects of image noise on the detection of motion-defined form depended on speed in a nonlinear fashion. At both the highest and lowest dot speed, performance declined more appreciably with increasing noise compared with the middle speeds. Thus, for a small SNR, the relation between detection performance and dot speed followed an inverted U-shaped function. The decline in performance at low speeds was evident at all SNR levels, while the upper decline was only seen with the smallest SNR levels.

The threshold image SNR required for detection at each dot speed was obtained by fitting cumulative normal functions to the data and interpolating the SNR necessary to correctly detect the motion-defined square at a level of 75%. As the lowest illumination level used was 100 (SNR of 0.23), when performance at this and higher levels exceeded threshold, the threshold was assigned by default to this minimum stimulus level (a floor effect). Fig. 4 illustrates that the threshold was lowest for the mid-speed ranges and was elevated at the lowest and highest speeds and repeated-measures analysis of variance confirmed a significant main effect for dot speed ($F(4, 57) = 43.93$, $p < 0.001$). There was no significant effect of motion type, but a nonsignificant tendency for the SBRS and MBRS conditions to have higher thresholds than the SBOS and MBOS conditions, particularly for the slowest dot speed. Whether the border was stationary or moving did not significantly affect detection performance. In a real-world scenario, this finding suggests that noise would impair the detection of camouflaged objects both when moving in the open and when moving behind stationary openings, such as through the canopy of a forest.

Nawrot *et al.* [41] estimated the proportion of signal dots in a motion-defined region required to segregate a motion-defined form. They found that the threshold proportion of signal dots required for motion-defined letter identification was lower for conditions analogous to our SBOS conditions (approximately 3%) compared with our SBRS conditions (approximately 22%). The discrepancy between the strong effect of the type of background motion in Nawrot *et al.*'s and the small effects in the present study might reflect the considerable differences in task or the fact that the dots in the former study moved at a speed (198 arcmin/s), where performance was typically above threshold at all noise levels tested in the current study (a floor effect).

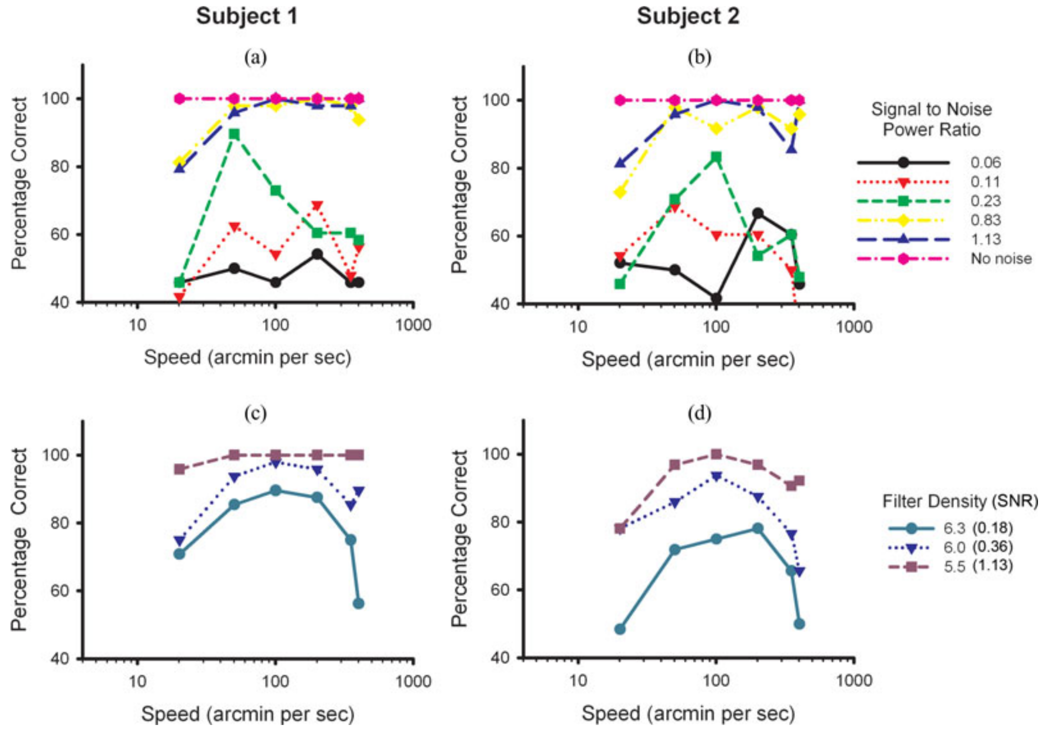

Fig. 5. Results of Experiment 2. Each curve represents percentage correct detection for a different noise condition as a function of dot speed. (a) and (b) Motion-defined square detection performance for Observers 1 and 2 using synthetic imagery averaged over the left and right eyes. (c) and (d). Performance using night vision devices (NVDs) for each observer averaged over the left and right NVD tubes. The equivalent SNR is listed for each filter density, assuming that the 5.5 filter is equivalent to an SNR of 1.13 (based on comparison with the simulated data). Note that the ratios between the SNR for the different filter conditions does not depend on this assumption.

IV. Experiment 2: Detection of a Motion-Defined Form Using Night Vision Devices

Experiment 1 demonstrated that performance on detection of motion-defined form was degraded as image noise increased and that this degradation was velocity specific—degrading relatively more at the lowest and possibly highest velocities tested compared with the middle range of speeds. In Experiment 2, we validated these results for motion-defined form detection through real NVDs.

A. Methods

Stimuli were similar to those used in Experiment 1 under the SBRS condition. The direction of the moving square was randomly selected from one of the four cardinal directions. Five levels of dot speed were used for both real and synthetic noises: 20.1, 50.4, 100.7, 201.4, 352.5, and 402.9 arcmin/s. Real and synthetic stimuli were presented in separate sessions in counterbalanced order.

As in Experiment 1, simulated NVD image noise was added to the motion-defined square stimuli in the synthetic imagery case. Image noise was present in all parts of the test stimuli arising implicitly from the model's response to a range of five input illuminations (25, 50, 100, 367, and 500 photons per pore per frame or equivalent SNR of 0.06, 0.11, 0.23, 0.83, and 1.13). Note that both the dot speed range and the SNR range were slightly larger than in Experiment 1 to investigate the limits of motion-defined form processing further.

The same procedure was used under the real-imagery condition, with the exception that noise-free stimuli were presented on the display, and noise was introduced into the images viewed by the observer through the NVD response to reduced illumination. We controlled illumination by placing broad-spectrum neutral density (the nominal attenuation was obtained near the 565 nm spectral emission peak of the display phosphor, absorption declined gradually with higher wavelengths over the spectrum from 400 to 1000 nm) filters in front of the NVD objectives and having observers view noise-free stimulus displays on the monitor. The neutral density filter values were 5.5, 6, and 6.3 (log attenuation) producing three levels of input illumination. SNR declines in NVDs as illumination decreases. Unlike the simulation, there is no discrete frame rate in the NVD, although the discrete microchannel plate pore array is somewhat analogous to the simulated pixels. The NVD used was a standard ANVIS-9 binocular NVG with generation III intensifier tubes (ITT Night Vision, Roanoke, VA 24019) focused at the distance of the screen.

Input illumination levels in both real and synthetic conditions were selected to ensure that a realistic range of values was tested. Under both conditions, stimuli were viewed monocularly (each eye or tube in separate sessions). Under a final control condition, observers directly viewed (synthetic) noise-free motion-defined squares that were presented at the same speeds as above.

B. Results and Discussion

For each observer, psychometric functions were obtained by plotting the total percentage of correct choices as a function of dot speed for each SNR level. Fig. 5(a) and (b) shows these psychometric functions for the synthetic condition, and Fig. 5(c) and (d) shows performance under the real condition, for two observers, respectively. In addition, performance for the no-noise imagery is plotted in the graphs of the simulated data. With no noise, observers achieved perfect performance across all motion speeds, demonstrating that detecting the motion-defined form in the stimulus was trivial when noise was not added to the stimuli. The noise-free condition also provided a baseline performance level to compare against all conditions in which input illumination was reduced (or effectively noise was added).

In keeping with the no-noise condition, uniformly high performance was found for the largest SNR levels in the synthetic condition. Both observers (and from both monocular views) demonstrated performance decrements across all dot speeds when the input light level equaled 100 photons per pore per frame or lower (SNR of 0.23 or lower). Performance at these lower simulated illumination levels was consistently worse than for high input illumination levels or when noise was not added to the imagery. Fig. 5(a) and (b) also shows that performance decrements were noticed across all input illumination levels for low dot speeds. Taken together, these findings were consistent with Experiment 1.

For the real imagery, the same general trends as were seen for the synthetic condition were found for both observers across both tubes. As shown in Fig. 5(c) and (d), a reduction in input illumination (increase in filter attenuation) produced a decrease in performance. An increased sensitivity to noise at both low and high dot speeds was apparent. It is important to note that there was a similar trend toward the reduced performance at high dot speeds under the synthetic condition, but it was less clear. In summary, these results showed that a reduction in input illumination level (i.e., increased noise), for both synthetic and real conditions, produced decrements in performance and these decrements depended on dot speed. These effects were exacerbated at low and, less consistently, high dot speeds and were consistent with Experiment 1.

The fact that similar results are shown with real NVD image conditions suggests that the synthetic imagery captures relevant features for the task.

V. Experiment 3: Effect of Noise Distribution

The previous experiments used Poisson-distributed noise to model the photon arrival statistics at the NVD input photocathode. In interpreting the results in terms of motion processing, it is important to assess the appropriateness of such a model. In terms of describing the effects of instrument noise on motion perception in NVDs and other devices, it is important to ensure that our conclusions are not overly sensitive to the particular noise model chosen, as the model is only an approximation of reality for NVDs and is not appropriate for many other devices. In terms of physiological relevance, measurement of neural or psychophysical responses to external noise is an important technique for characterizing human visual processing and internal noise processes. While Poisson processes are suitable models of discrete processes in the visual system such as retinal photon arrival [11] or spike generation processes [12], [13] many models of visual system noise use other statistical distributions. As signal level increases, the central limit theorem implies that many noise distributions will approximate a Gaussian distribution and such a distribution is central to many neural modeling efforts. Thus, it is important to study whether our findings apply with other noise processes, particularly Gaussian.

Another possible mechanism for the influence of noise on the detection of motion-defined form is the disruption of motion correspondences [12], [14]. That is, the noise might effectively degrade spatio-temporal correlation and make establishment of correspondence between dot elements on subsequent frames difficult.

Thus, in this experiment, we evaluated the sensitivity of our results 1) to the particular noise distribution modeled by comparing performance in the presence of Poisson and Gaussian noise distributions and 2) in the presence of explicit dot decorrelation rather than additive noise. Finally, we also increased the range of dot speeds tested to more closely examine the fall off in performance at higher dot speed found in Experiments 1 and 2.

A. Methods

The procedure and observer task were identical to the synthetic conditions in Experiments 1 and 2 except the stimulus duration was 100 ms rather than 250 ms. Motion-defined targets were created by moving one central patch of dots in one of the four cardinal directions with the surround dots in random motion (SBRS condition). Several levels of dot speed were used for each type of synthetic noise: 10.1, 20.1, 50.4, 100.7, 201.4, 402.9, 805.7, and 1208.6 arcmin/s. We also tested observers at a dot speed of 1611.4 arcmin/s with the Poisson distributed noise to investigate the high dot speed fall off further.

Three different noise conditions were studied namely Poisson, Gaussian, and decorrelation noises. As in Experiments 1 and 2, for Poisson noise conditions simulated NVD image noise was added to these motion-defined square stimuli using [9] model at three input illuminations (100, 500, and 1000 photons per pore per frame or SNR of 0.23, 1.13 and 2.25). Under the Gaussian noise conditions, normally-distributed additive image noise was added (SNR of 0.23, 1.13, and 2.25 expressed in terms of the ratio of signal power to noise variance). Decorrelation noise was achieved by adding a number of randomly placed dots on each frame. Contrast on every frame of the decorrelated stimulus was maintained across the different noise levels because additional high contrast dots were added. However, because a different sample was selected on each frame the result was a scintillating perception and a perception of reduced contrast. On each frame, either 2000, 12000, or 16000 dots were placed in random positions giving a decorrelated dot to signal dot ratio of 0.5, 3.0, and 4.0.

B. Results and Discussion

As in the previous experiments, an increase in Poisson noise resulted in a decrease in detection performance (see Fig. 6). As found previously, this was most pronounced for the highest and lowest dot motion speeds (inverted u-shape). The proportion of correct responses varied significantly with dot speed for all SNR levels except the lowest (SNR 0.23: $\chi^2(8) = 13.70$, $p = .180$, all

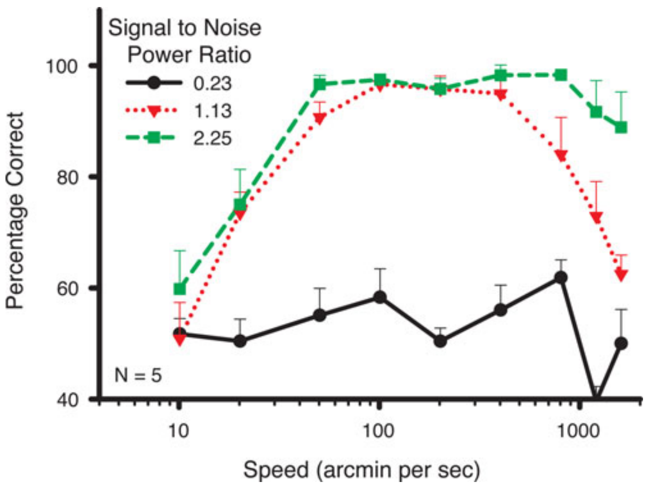

Fig. 6. Motion-defined form detection in the presence of Poisson image noise. Each curve represents percentage correct detection (+s.e.m.) for a different signal to noise ratio condition as a function of dot speed.

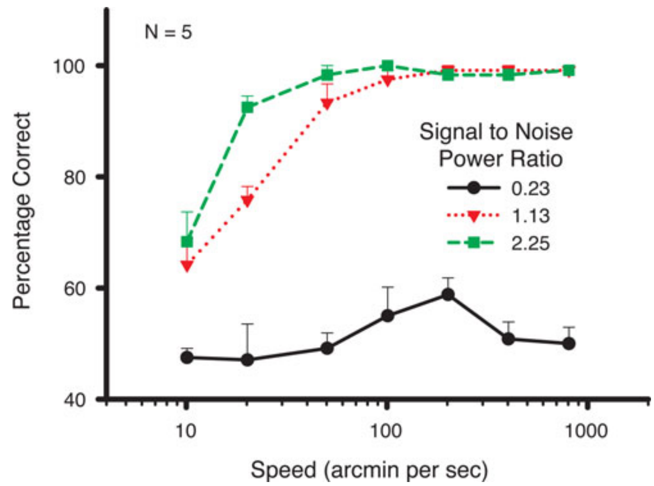

Fig. 7. Motion-defined form detection in the presence of Gaussian image noise. Each curve represents percentage correct detection (+s.e.m.) for a different signal to noise ratio condition as a function of dot speed.

p-values adjusted for multiple comparisons; SNR 1.13: $\chi^2(8) = 156.25$, $p < .001$; SNR 2.25: $\chi^2(8) = 170.42$, $p < .001$). For the higher two SNRs, the fall offs at higher and lower velocities are apparent and performance is significantly degraded compared with middle speeds. The higher dot velocity falloff is more apparent in Fig. 6 compared with Fig. 3 since the upper range of dot velocity was increased in the current compared with the previous experiment. The fall off is also more pronounced with higher image noise (performance is significantly better at SNR of 2.25 compared with 1.13 at speeds of 805.7 arcmin/s and higher, $p < .01$). Performance for the lowest simulated illumination/ highest noise (SNR of 0.23) was poor across all stimulus velocities and was generally poorer than found in the earlier experiments for this condition, perhaps due to the briefer stimulus exposure in the present experiment.

An unexpected observation was the similarity of the data for 1.13 and 2.25 SNR at the lower velocities. In particular, the average performance for the 20 arcmin/s, 2.25 SNR condition seemed relatively poor. Two of the subjects demonstrated an increase in performance from near chance values at a slightly higher velocity than the others (between 20 and 50 arcmin/s rather than between 10 and 20 arcmin/s). In fact, these two subjects showed nominally poorer performance with an SNR of 2.25 than an SNR of 1.13 at 20 arcmin/s, which reduced the average performance for the 2.25 SNR condition.

An increase in Gaussian-distributed noise also produced a decrease in performance (see Fig. 7). The proportion of correct responses was found to vary significantly with dot speed for all SNR levels except the lowest, where performance was uniformly poor (SNR 0.23: $\chi^2(6) = 5.21$, $p = .75$; SNR 1.13: $\chi^2(6) = 155.01$, $p < .001$; SNR 2.25: $\chi^2(6) = 155.36$, $p < .001$). The speed dependence was most evident at low dot speeds with signs of a nonsignificant trend to high-speed falloff only apparent at the lowest SNR. Performance at low speeds was significantly worse than at mid speeds for the 1.13 and 2.25 SNR. The low speed falloff appeared stronger for noisier image sequences (performance at 20.1 arcmin/s was significantly poorer for the 1.13 compared with 2.25 SNR, $\chi^2(1) = 11.29$, $p = .0019$). The lack of a falloff at the highest speeds may be due to the fact that the effective noise level may have been less in the Gaussian case. Note that we used the noise power in the background for characterizing the Poisson noise power. As the variance of a Poisson random process is proportional to its intensity, the variability in the brighter dots is larger than in the background (in absolute terms). Thus, the noise may be effectively larger in the Poisson case than in the Gaussian case (where the same noise distribution is added to both signal and background), despite equating the SNR.

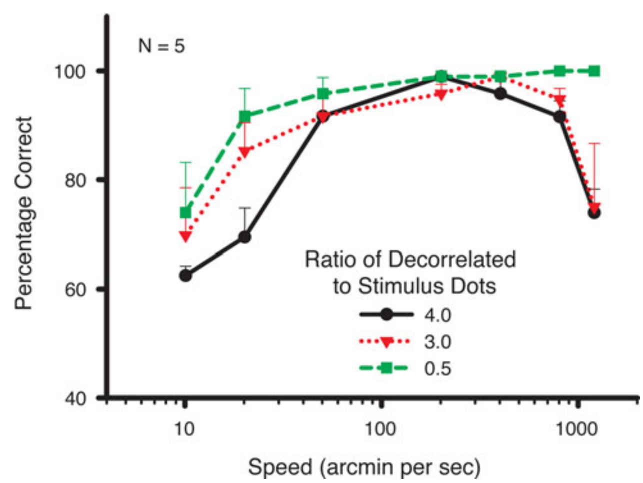

Fig. 8. Motion-defined form detection in the presence of image decorrelation noise. Each curve represents percentage correct detection (+s.e.m) for a different decorrelation condition as a function of dot speed.

Motion-defined form detection in the presence of decorrelation noise is shown in Fig. 8. As the number of decorrelated dots increased, performance declined but only at the lowest and highest dot speeds. The curves were qualitatively very similar to those for the Poisson distributed noise in Fig. 6, and the NVD results in experiment 2 including the inverted U-shape of the psychometric function. The proportion of correct responses was

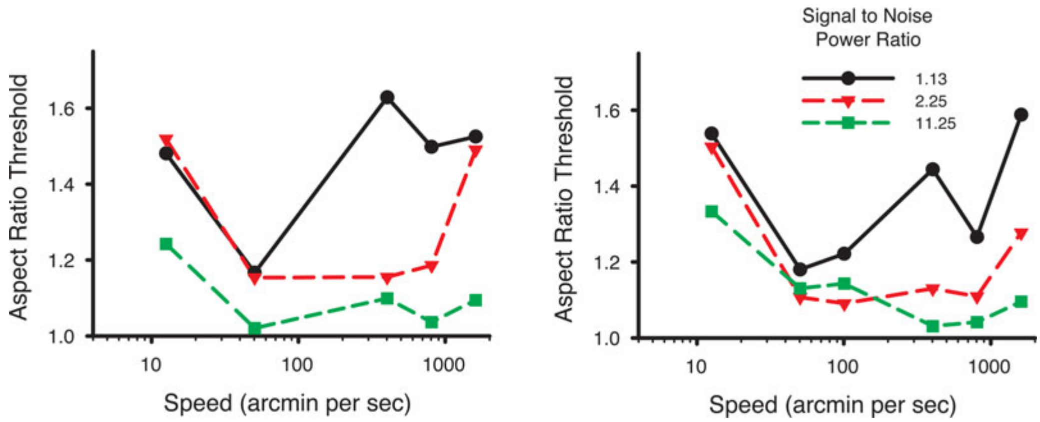

Fig. 9. Motion-defined form discrimination for two observers in the presence of Poisson image noise. Each curve represents the threshold (79% correct) for discriminating rectangle aspect ratio for different levels of Poisson signal to noise ratio as a function of dot speed.

found to vary significantly with dot speed for all the noise levels (ratio of noise to signal dots 0.5: $\chi^2(6) = 92.74$, $p < .001$; 3.0 ratio: $\chi^2(6) = 64.50$, $p < .001$; 4.0 ratio: $\chi^2(6) = 86.75$, $p < .001$). Performance at the middle speeds was fairly constant but at the lowest 10.1 arcmin/s dot speed performance was significantly poorer than at either 20.1 or 50.4 arcmin/s for all noise-to-signal dot ratios. At the highest 1208.6 arcmin/s dot speed, performance was significantly reduced compared with performance at 805.7 arcmin/s but only for the two highest noise levels ($p < .01$). The inverted U-shape appeared more pronounced as noise level increased, with performance rising more slowly at low speed (performance at 20.1 arcmin/s was significantly worse at the 4.0 noise to signal dot ratio than at both the 0.5 and 3.0 ratios, $p = .0013$ and $p = .05$, respectively) and falling more rapidly at higher velocities (performance at 1208.6 arcmin/s was significantly worse at both the 3.0 and 4.0 noise-to-signal dot ratios than at the 0.5 ratio, $p < .001$ for both cases). It is difficult to quantify the degree of decorrelation that is caused by the continuous additive luminance noise as dots may be degraded but still present in the presence of luminance noise (or a spurious "dot" may be created but at a low intensity level). However, the striking similarity between the additive noise and decorrelation results suggests that the disruption of motion correspondence may play a major role in the difficulty in perceiving motion-defined form in the presence of noise.

VI. Experiment 4: Discrimination of a Motion-Defined Form

Even in normal viewing, motion detection mechanisms must exhibit tolerance to noise due to neuronal variability, the aperture problem (leading to uncertainty on local estimates of motion direction and magnitude), and correspondence noise. Spatial pooling can temper the effects of local noise and improve the reliability of the pooled motion signal, but pooling can also degrade the ability to segregate local motion signals [15]. Pooling mechanisms likely differ for different motion tasks; for example, Watamaniuk and Sekuler [16] claimed spatial integration was very large and estimated an area of 63 deg^2 for global direction discrimination, whereas Regan and Beverley [17] estimated much smaller foveal summation fields ($0.16\ deg^2$) for motion-defined form detection. The latter were large compared with those for luminance-defined form but still would provide for precise estimation of object boundaries. Van Doorn and Koenderink [18] have shown that, although the detection of correlation in motion-defined forms is possible in short, thin strips, increasing stimulus size improves performance due to spatial pooling.

In our stimuli, pooling would improve the reliability of the motion signals in the target and surround but would interfere with the differential processing required to segment the target from surround. In the previous three experiments, subjects detected the presence of a motion-defined object. This task required the segregation and detection of motion signal differences but did not necessarily require that the subjects have an accurate percept of the shape of the stimulus. In the final experiment, we study the effects of noise on the ability to discriminate the shape of a motion-defined form.

A. Methods

The stimuli and procedures were similar to the previous experiments with the following differences. Instead of a $4.3° \times 4.3°$ central motion-defined square, we used a rectangular motion-defined form whose aspect ratio varied from 1.0 (a 4.3° x 4.3° square) to 2.5 (highly rectangular, either "fat" or "narrow"), trial to trial. The total area was kept constant. In Fig. 9, aspect ratio is expressed as the ratio of the larger side over the smaller side to express the "fat" and "narrow" stimuli in equivalent rather than reciprocal terms.

A single 100-ms image sequence was presented on each trial. Following each trial, observers indicated whether the rectangle was "fat or "narrow" with key presses. Interleaved staircases were used to estimate the aspect ratio threshold at 79% correct using the three-up, one-down method of Levitt (1971) for each noise condition as a function of speed. Four staircases were used and pseudorandomly interleaved, targeting the thresholds for both "fat" and "thin" aspect ratios and starting either well below threshold or well above threshold.

B. Results and Discussion

Consistent with the literature, under low-noise conditions and moderate speeds subjects could discriminate aspect ratio differences of a few percent [19]. As SNR decreased aspect ratio thresholds increased. At the lowest dot speed, thresholds were elevated by 20% or more compared with the next highest speed. Thus, performance degraded at the lowest speed regardless of noise level. In contrast, noise had a selectively detrimental effect at the highest speeds. At the highest speeds, thresholds rose very little for the highest SNR condition and substantially for the lowest SNR levels. A ceiling effect was evident in one of the observer's data and the highest thresholds reached were no greater than about 1.6 (this was a very extreme aspect ratio of more than 3:2).

In sum, as for motion-defined form detection in Experiments 1–3, the ability to discriminate a motion-defined form followed a U-Shaped profile with greatest detrimental effects at high and low dot speeds. In the present experiment, the low-speed decrement in performance was not image noise level dependent and may be a general difficulty in discriminating the motion-defined form with small relative velocity signals [17]. In contrast, the noise-dependent discrimination deficit found at higher dot speed might have important human factors implications: it predicts deficits in the discrimination of the motion-defined form due to NVD noise that occur at image velocities where observers may have an expectation of high sensitivity based on their daylight vision experience.

VII. General Discussion

The addition of simulated or real image noise reduced the performance of motion-defined form detection and discrimination, particularly at low and high dot velocity. These findings have implications for the usability of displays in the presence of noise and for the nature of processing of motion-defined form in the human visual system.

Performance on apparent motion tasks in random-dot displays is degraded if interframe dot displacement is either too small or too large, quantified by performance thresholds $D_{\min}$ and $D_{\max}$, respectively [20]. In the present study, the influence of added noise was most pronounced at the lowest and highest target speeds. In other words, the addition of noise caused elevation of $D_{\min}$ and reduction of $D_{\max}$. Reduction in $D_{\max}$ may reflect interference with fundamental motion processes as discussed next.

Several factors may contribute to difficulty in processing noisy image sequences, including 1) effects of noise on $D_{\max}$ and $D_{\min}$; 2) effective contrast reduction (or reduction in effective spatial sampling rate) degrading the visibility of target features; 3) pooling and spatial averaging (or similar strategies) for noise suppression interfering with the ability to segregate figure and ground; and 4) decorrelation due to noise interfering with or degrading the matching process.

A. Effects of Noise on $D_{\max}$ and $D_{\min}$

Van Doorn and Koenderink [18] performed the most directly comparable study to the experiments described here. Their observers adjusted the contrast of a temporally correlated, stroboscopically moving pattern relative to that of a superimposed, temporally uncorrelated noise pattern (with overall contrast held constant) in a target region until the target could just be detected against a background of temporally uncorrelated noise. The binary noise used is most like our decorrelation condition although the noise contrast varied as in our additive noise stimuli. Consistent with our finding that less noise was tolerated at higher dot velocities, van Doorn and Koenderink reported that the threshold SNR increased with the velocity of the moving signal at the higher end of their velocity range.

However, in their experiments there was no increase in sensitivity to noise at low velocities, which is inconsistent with our results. While the stimuli differed in many respects (e.g., high versus moderate density, binary versus Poisson noise), this difference in noise sensitivity is most likely due to differences in task requirements. In the van Doorn and Koenderink study, the subject simply needed to detect the correlated signal, which could be done efficiently even with a stationary stimulus. In contrast, the detection task in this study requires segregating motion-defined areas based on differential motion, which is made easier by increased motion contrast. With a stationary or slowly moving stimulus there would be simply no motion signal available to support segregation and thus performance should be influenced by the presence and rate of motion.

Most studies of $D_{\max}$ are based on apparent motion sequences, often only two frame stimuli so the relevance to smooth motion displays might be questioned. Snowden and Braddick [21] showed that $D_{\max}$ increased with the number of frames in an apparent motion sequence. De Bruyn and Orban [22], using strobed continuous motion displays, found that exceeding a maximum interflash (or interframe) displacement still caused a decrement in discrimination performance, despite the transition from strobed motion to the perception of smooth, flicker-free, continuous motion. From their data (their Fig. 2), we can extrapolate a $D_{\max}$ of 30–35 arcmin or equivalently a $V_{\max}$ of 3000–3500 arcmin/s for our 4.3° width (target region), 100 Hz stimuli. Similar estimates have been made for $D_{\max}$ when discriminating the orientation of a motion-defined form in an extended apparent motion sequence [23]. This velocity is much higher than we tested and in accordance, we found that performance with noise-free stimuli showed no sign of approaching $D_{\max}$.

B. Effective Contrast

The NVG model and the real NVGs incorporated automatic gain control to normalize the image intensity and hence mean luminance did not vary significantly across conditions in our experiments. This combined with the relatively weak effects of luminance on $D_{\max}$ [24], [25] suggests that luminance is not a significant factor in these experiments.

While Dawson and Di Lollo [24] found that $D_{\max}$ was not affected by stimulus contrast, contrast does have a demonstrated impact on motion sensitivity, $D_{\min}$ [26]. Therefore, we might expect that effective contrast reduction with increasing noise would have had an influence particularly for the detection of slowly moving stimuli. However, the effect of contrast on $D_{\min}$ appears to saturate rapidly with contrast, reaching asymptotic levels at low (2–6%) contrast [27], [28] possibly due to contrast gain control [26]. Therefore, we should expect contrast effects on the motion-defined form detection to occur only for high noise conditions and at low speeds.

The results of Experiment 3 also suggest that instantaneous contrast reduction cannot fully explain our results. Contrast on every frame of the decorrelated stimulus was maintained across the different noise levels since additional high contrast dots were added. The fact that a similar pattern of results was found for the decorrelation and additive noise conditions suggests that instantaneous contrast was not a key factor. However, even in the decorrelation case, the noise was dynamic and would be neurally integrated over multiple frames, which results in a reduction in perceived contrast. Regan and Beverley [17] estimated a temporal integration time constant of 750 ms for motion-defined form discrimination. Such a long time constant would imply that the motion information would be integrated over most if not all of our stimulus presentation. Futhermore, motion coherency has been shown to be sensitive to contrast over a larger range than direction discrimination (see Section VII-D), opening the possibility for interaction between contrast and decorrelation as a factor limiting motion-defined form perception in noise.

C. Pooling and Spatial Averaging

Spatial pooling reduces the effects of random noise, but can interfere with the differential processing required to segment the target from background. For the motion-defined form detection task, this segmentation could possibly be done in a coarse fashion. However, for *discrimination* of a motion-defined form, the small aspect ratio thresholds of a few percent obtained suggest that the pooling is either well matched to the target area or at a fine enough scale to preserve a clear outline of the shape, at least under low-noise conditions [17]. Reduction of performance with increased noise in the discrimination task could reflect the increased need for pooling of signals over larger spatial extents consequently degrading the ability to sharply segregate the target from background. At the lowest speeds, the motion signal is weak and more pooling might be required. At the higher speeds, we might see reductions in $D_{\max}$ degrading performance as discussed previously. However, pooling may play a role here as well. Many investigators have suggested a correlation between the scale of motion detector mechanisms and their displacement range [29]. Presumably pooling of large scale mechanisms is coarser than pooling of fine scale mechanisms and, if so, the impact of increased spatial pooling may be more apparent at large displacement than at moderate.

D. Effects of Decorrelation

Noise can result in decorrelation by interfering with the matching process establishing correspondence between features across time. This could be due to 1) increased variability in the intensity of target dots which could interfere with matching and/ or introduce noise into velocity estimation or 2) spurious matching between noise elements or between noise and signal elements that would reduce coherence and introduce flicker and noisy motion signals.

The distinction between "informational" [29], [30] and "filter" approaches to establishing temporal correlation and motion estimation has been debated vigorously in the literature [31]. For our purposes, in both views motion detectors are sensitive to spatiotemporal correlation between frames in the image sequence and would be disrupted by spatiotemporal noise producing false matches or alternatively motion energy away from the true target motion.

Our finding that decorrelation noise produces similar patterns of results to additive, scintillating noise suggests that correspondence noise is a critical factor in the effects of noise on $D_{\max}$ and $D_{\min}$ found in this study. Dots that are incorrectly matched reduce the coherence of the motion signal. Transient noise dots that are not matched will provide weak and incoherent motion signals. Transient noise dots matched to noise or signal dots on another frame will also reduce the coherence of the motion signal. The effects of motion noise from dots appearing and disappearing at random positions on each frame seems to be quantitatively comparable to decoherence from randomly moving dots [32].

Todd and Norman [23] measured the detection of coherent motion in a rectangular aperture in a two-alternative forced choice task. In one experiment, a temporally uncorrelated noise pattern was presented in one aperture and an extended or two-frame sequence of apparent motion (with or without noise or transparent motion) in the other aperture. When the motion signal was superimposed with an equal number of temporally uncorrelated dots, $D_{\max}$ was lower than for a unidirectional motion signal alone. This noise condition is similar to our decorrelation condition and suggests that $D_{\max}$ for global motion direction discrimination is also limited by false matching.

Edwards *et al.* [33] have reported that motion coherence varies with contrast and further that the contrast saturation depends on the difficulty of the task. They argued that the saturation with contrast reflects performance ceilings rather than limitations on the contrast response of the motion mechanisms themselves. Thus, it is possible that reduction in effective contrast under the additive noise conditions may have compounded the effects of decorrelation, but further investigation would be required to determine the relative and combined effects of decorrelation and contrast reduction.

E. Noise Characterization and Modeling

Glasgow *et al.* [34] recently characterized NVD image noise by comparing a series of real NVD displays to a simulated (e.g., computer-generated) NVD environment. Their findings quantified several perceptual characteristics of NVD image noise using subjective measures. Generally, the dominant noise sources are Poisson [9], [35], [36], although other noise sources exist such as the fixed pattern noise due to the grid spacing of the fibers in the inverting optics of the goggles used in this experiment. The close qualitative agreement in the pattern of the results obtained with real and simulated NVG noise in this study suggests that the Poisson noise parameters did model the key characteristics of the effect of image intensifier noise on motion-defined form.

F. Generalization of the Findings

As is typical in the field of motion psychophysics, our study relied on repeated measurements over many trials to collect precise measurements on a small number of young, healthy observers paying careful attention to the task (e.g., [19], [21], and [27]). This allows for sensitive estimation of the effects, but we need to be cautious extrapolating to larger samples. Experiments on motion-defined form perception using the procedures adapted for large subject samples shows that subjects typically have similar performance patterns and that selective deficits in these patterns can be associated with disease [37]. This combined with the fact that we were studying the effect of device not observer characteristics suggests that the results should generalize to a broader population, although absolute sensitivity of individuals will vary.

G. Implications for Flight

Motion perception is an important visual process during night flight operations. For example, motion information can help pilots identify and recognize moving targets on the ground and can facilitate camouflage breaking. Motion is useful for these tasks because it facilitates the perception of the form of a target and its segregation from the background based on differential motion. We studied the capacity to detect motion-defined form under simulated and real NVD conditions. Our results are consistent with pilot reports that they have greater difficulty using visual motion cues under low levels of night-time illumination.

Our tests were conducted with real or simulated monocular NVD devices, whereas many operational systems are binocular. One would expect that the correlation of the signal and independence of the noise in the two channels would permit improved performance with binocular viewing, but this needs to be experimentally confirmed.

The current results show that image noise reduces the effectiveness of motion as a viable cue to object detection and segmentation. Image noise would have the greatest effects at low ambient illumination when devices have the highest gain settings and consequently the highest noise levels. We found that the capacity to detect a motion-defined form was impaired under low levels of illumination under both simulated and real NVD conditions. These deficits likely impact flight performance. For example, they may influence the pilot's ability to do collision detection/avoidance and route planning during low-level flight although it is difficult to predict which particular flight tasks might be most affected (e.g., formation flight, cruise at altitude, nap-of-the-earth flight, and hover or landing [38]. Beyond form from motion processing, image noise may affect other important aspects of motion perception including speed judgment, motion segregation, judgments of heading or self-motion from optic flow, or the ability to use motion parallax as a cue to depth and structure.

The effects of NVD image noise can be reduced through device improvements, digital image processing, procedural solutions such as flight restrictions based on ambient luminance levels, and improved training protocols. As the civilian use of night-vision devices increases, reassessment of standard operating procedures and guidelines designed for military aviation is required to ensure the safe and effective use of the devices in civilian aviation. For example, airborne law enforcement agencies frequently need to track moving vehicles and targets using NVDs under a range of illumination. Appreciation of the difficulties in detecting the motion-defined form under noisy conditions could help optimize operational protocols. Similarly, incorporating realistic noise levels in NVD simulations may improve trainees' understanding of perceptual limitations in operational contexts. Rational engineering and operational decisions depend on identifying where motion perception degrades in order to define the requisite training protocols and enhance the efficiency and safety level of night flying.

Acknowledgment

The authors would like to thank P. Guterman for assistance in testing observers and collecting data, C. Hylton for assistance in the preparation of the manuscript, I. Tsang for assistance with programming, and L. Wilcox for helpful comments. Portions of this work have been reported at conferences [39], [40].

References

[1] D. Regan, *Human Perception of Objects : Early Visual Processing of Spatial Form Defined by Luminance, Color, Texture, Motion, and Binocular Disparity*. Sunderland, MA, USA: Sinauer Associates, 2000.

[2] H. B. Barlow, "Measurements of quantum efficiency of discrimination in human scotopic vision," *J. Physiol.-Lond.*, vol. 160, no. 1, pp. 169–188, 1962.

[3] M. G. Braithwaite, P. K. Douglass, S. J. Durnford, and G. Lucas, "The hazard of spatial disorientation during helicopter flight using night vision devices," *Aviat. Space Environ. Med.*, vol. 69, no. 11, pp. 1038–1044, 1998.

[4] S. J. Durnford, J. S. Crowley, N. R. Rosado, J. Harper, and S. Deroche, "Spatial disorientation: A survey of U.S. Army helicopter accidents 1987–1992," Army Aeromedical Research Laboratory, Fort Rucker AL, Rep. AS-A298147, 1995.

[5] F. H. Durgin and D. R. Proffitt, "Perceptual adaptation in the use of night vision goggles," NASA, Charlottesville, VA, USA, Rep.. NAG2–721, 1992.

[6] F. H. Durgin and D. R. Proffitt, "Perceptual Response to visual noise and display media [Final Report]," NASA, Charlottesville, VA, USA, Rep. NAG2–814, 1993.

[7] J. T. Riegler, J. D. Whiteley, H. L. Task, and J. C. Schueren, "The effect of signal-to-noise ratio on visual acuity through night vision goggles," Armstrong Laboratory, Rep. AL-TP-1991—0011, 1990.

[8] A. Rivamonte, "Resolution and signal-to-noise measurement US Army night vision goggles," *Proc. SPIE*, vol. 1290, pp. 206–215, 1990.

[9] P. J. Thomas, R. S. Allison, S. Jennings, K. Yip, E. Savchenko, I. Tsang, T. Macuda, and R. Hornsey, "Validation of synthetic imagery for night vision devices," *Proc SPIE*, vol. 5442, pp. 25–35, 2004.

[10] A. Bradley and M. K. Kaiser, "Evaluation of visual acuity with gen III night vision goggles," *National Aeronautics andSpace Administration*, Rep. N94–23974, Jan. 1994.

[11] H. B. Barlow, W. R. Levick, and M. Yoon, "Responses to single quanta of light in retinal ganglion cells of the cat," *Vis. Res.*, vol. 11, pp. 87–101, 1971.

[12] S. C. Dakin, I. Mareschal, and P. J. Bex, "Local and global limitations on direction integration assessed using equivalent noise analysis," *Vis. Res.*, vol. 45, no. 24, pp. 3027–3049, 2005.

[13] M. N. Shadlen and W. T. Newsome, "Noise, neural codes and cortical organization," *Curr. Opin. Neurobiol.*, vol. 4, no. 4, pp. 569–579, Aug. 1994.

[14] J. S. Lappin and H. Bell, "The detection of coherence in moving random-dot patterns," *Vis. Res.*, vol. 16, no. 2, pp. 161–168, 1976.

[15] O. Braddick, "Segmentation versus integration in visual motion processing," *Trends Neurosci.*, vol. 16, no. 7, pp. 263–268, Jul. 1993.

[16] S. N. Watamaniuk and R. Sekuler, "Temporal and spatial integration in dynamic random-dot stimuli," *Vis. Res.*, vol. 32, no. 12, pp. 2341–2347, 1992.

[17] D. Regan and K. I. Beverley, "Figure-ground segregation by motion contrast and by luminance contrast," *J. Opt Soc. Amer. A*, vol. 1, no. 5, pp. 433–442, May 1984.

[18] A. J. Van Doorn and J. J. Koenderink, "Spatiotemporal integration in the detection of coherent motion," *Vis. Res.*, vol. 24, no. 1, pp. 47–53, 1984.

[19] D. Regan and S. Hamstra, "Shape discrimination for motion-defined and contrast-defined form: Squareness is special," *Perception*, vol. 20, no. 3, pp. 315–336, 1991.

[20] O. Braddick, "A short-range process in apparent motion," *Vis. Res.*, vol. 14, no. 7, pp. 519–527, 1974.

[21] R. J. Snowden and O. Braddick, "Extension of displacement limits in multiple-exposure sequences of apparent motion," *Vis. Res.*, vol. 29, no. 12, pp. 1777–1787, 1989.

[22] B. De Bruyn and G. A. Orban, "Discrimination of opposite directions measured with stroboscopically illuminated random-dot patterns," *J. Opt. Soc. Amer. A, Opt. Image Sci.*, vol. 6, no. 2, pp. 323–328, 1989.

[23] J. T. Todd and J. F. Norman, "The effects of spatiotemporal integration on maximum displacement thresholds for the detection of coherent motion," *Vis. Res.*, vol. 35, no. 16, pp. 2287–2302, 1995.

[24] M. Dawson and V. Di Lollo, "Effects of adapting luminance and stimulus contrast on the temporal and spatial limits of short-range motion," *Vis. Res.*, vol. 30, no. 3, pp. 415–429, 1990.

[25] M. J. M. Lankheet, A. J. van Doorn, and W. A. van de Grind, "Spatiotemporal tuning of motion coherence detection at different luminance levels," *Vis. Res.*, vol. 42, no. 1, pp. 65–73, Jan. 2002.

[26] B. L. Beard, S. A. Klein, and T. Carney, "Motion thresholds can be predicted from contrast discrimination," *J. Opt. Soc. Amer. A*, vol. 14, no. 9, pp. 2449–2470, Sep. 1997.

[27] M. J. Morgan, R. Perry, and M. Fahle, "The spatial limit for motion detection in noise depends on element size, not on spatial frequency," *Vis. Res.*, vol. 37, no. 6, pp. 729–736, Mar. 1997.

[28] K. Nakayama and G. H. Silverman, "Detection and discrimination of sinusoidal grating displacements," *J. Opt Soc Amer. A*, vol. 2, no. 2, pp. 267–274, Feb. 1985.

[29] M. J. Morgan and M. Fahle, "Effects of pattern element density upon displacement limits for motion detection in random binary luminance patterns," *Proc R. Sco. Lond., B*, vol. 248, no. 1322, pp. 189–198, May 1992.

[30] R. A. Eagle and B. J. Rogers, "Motion detection is limited by element density not spatial frequency," *Vis. Res.*, vol. 36, no. 4, pp. 545–558, Feb. 1996.

[31] T. Sato, "Dmax: Relations to low-and high-level motion processes," in *High-Level Motion Processing: Computational, Neurobiological, and Psychophysical Perspectives*, T. Watanabe, Ed. Cambridge, MA, USA: MIT Press, 1998, pp. 115–151.

[32] M. O. Scase, O. Braddick, and J. Raymond, "What is noise for the motion system?," *Vis. Res.*, vol. 36, no. 16, pp. 2579–2586, Aug. 1996.

[33] M. Edwards, D. Badcock, and S. Nishida, "Contrast sensitivity of the motion system," *Vis. Res.*, vol. 36, no. 16, pp. 2411–2421, 1996.

[34] R. L. Glasgow, P. L. Marasco, P. R. Havig, G. L. Martinsen, G. A. Reis, and E. L. Heft, "Psychophysical measurement of night vision goggle noise," in *Proc. Helmet- Head-Mounted Displays VIII: Technol. Appl.*, vol. 5079, Orlando, FL, USA., 2003, pp. 164–173.

[35] R. L. Bell, "Noise figure of the MCP image intensifier tube," *IEEE Trans. Electron. Devices*, vol. 22, no. 10, pp. 821–829, Oct. 1975.

[36] J. G. Wales and P. L. Marasco, "Statistical assessment of night vision goggle noise," *Proc SPIE*, vol. 6224, no. 1, pp. 62240I–62240I-12, May 2006.

[37] D. Regan and X. H. Hong, "Visual acuity for optotypes made visible by relative motion," *Optom. Vis. Sci*, vol. 67, no. 1, pp. 49–55, 1990.

[38] D. Regan, "Spatial orientation in aviation: visual contributions," *J. Vestib. Res.*, vol. 5, no. 6, pp. 455–71, 1995.

[39] T. Macuda, R. S. Allison, P. J. Thomas, G. Craig, and S. Jennings, "Detection of motion-defined form under simulated night vision conditions," *Proc. SPIE*, vol. 5442, no. 1, pp. 36–44, Sep. 2004.

[40] T. Macuda, G. Craig, R. S. Allison, P. Guterman, P. Thomas, and S. Jennings, "Detection of motion-defined form using night vision goggles," *Proc. SPIE*, vol. 5800, no. 1, pp. 1–8, May 2005.

[41] M. Nawrot, E. Shannon, and M. Rizzo, "The relative efficacy of cues for two-dimensional shape perception," *Vision Res.*, vol. 36, no. 8, pp. 1141–1152, 1996.

Robert S. Allison (SM'08) received the B.A.Sc. in computer engineering from the University of Waterloo, Waterloo, ON, Canada, in 1991, the M.A.Sc. in electrical engineering (biomedical engineering) from the University of Toronto, Toronto, ON, in 1994, and the Ph.D. degree specializing in stereoscopic vision from York University, Toronto, in 1998.

He is an Associate Professor of computer science and engineering with York University in Toronto joining the faculty in 2001. He is also appointed to the graduate program in psychology at York. He was on the experimental team for the 1998 Neurolab space shuttle mission and did Postdoctoral research with York University and the University of Oxford. Rob works on perception of space and self-motion in virtual environments, the measurement and analysis of eye-movements and stereoscopic vision. His research enables effective technology for advanced virtual reality and augmented reality and for the design of stereoscopic displays.

Dr. Allison is a member of the IEEE Computer Society and the Association for Computing Machinery.

Todd Macuda reeived the Ph.D. degree in neuroscience from the University of Western Ontario, London, ON, Canada, in 2000.

He is owner and Vice-President at Whistler Films, Kanata, Ontario, Canada. He is an Entrepreneur, Professor, Writer, and Film Producer. He began his career in academia as a Researcher and later accepted a position as a National Defence Scientist managing defence and aerospace development programs for the Canadian Federal Government. He launched his entrepreneurial career commercializing technologies and raising millions of dollars in capital for a wide range of aerospace and defence start-ups holding executive positions in business development, technology, and operations. In the business development role, he took ideas from infancy to realization exploiting markets and building companies. He is an Adjunct Professor and is active in supporting the development of scientific literacy in youth.

Dr. Macuda is also a member of the International Knightly Order of St. George and is involved in a range of charitable activities that support the Canadian military.

Sion Jennings received the B.A.Sc in chemical engineering in 1989, and the M.A.Sc in systems design engineering in 1992, both from the University of Waterloo, Waterloo, ON, Canada.

He is a Researcher with the National Research Council of Canada, Montreal, QC, Canada. He investigates aviation applications of new display systems.